Dalton Transactions

Synthesis, Characterization, and Alkoxide Transfer Reactivity of Dimeric Tl2(OR)2 Complexes

Journal:	*Dalton Transactions*
Manuscript ID	DT-ART-11-2020-003917.R2
Article Type:	Paper
Date Submitted by the Author:	16-Jan-2021
Complete List of Authors:	Groysman, Stanislav; Wayne State University, Chemistry Grass, Amanda; Wayne State University, Chemistry Wannipurage, Duleeka; Wayne State University, Chemistry Wathsala Kulathungage, Lakshani; Wayne State University, Chemistry Yousif, Maryam; Grand Valley State University Ward, Cassandra; Wayne State University

Synthesis, Characterization, and Alkoxide Transfer Reactivity of Dimeric $Tl_2(OR)_2$ Complexes

Amanda Grass,[a†] Lakshani Wathsala Kulathungage,[a†] Duleeka Wannipurage,[a†] Maryam Yousif,[c] Cassandra L. Ward,[b] Stanislav Groysman*[a]

[a]Department of Chemistry, Wayne State University, 5101 Cass Ave. Detroit MI 48202.

[b]Lumigen Instrument Center, Wayne State University, 5101 Cass Avenue, Detroit, Michigan 48202, United States.

[c]Current affiliation: Department of Chemistry, Grand Valley State University. 1 Campus Drive, 312 Padnos Hall

Allendale, Michigan 49401

E-mail: groysman@wayne.edu

[†]These authors contributed equally to this work.

Abstract

Reaction of $LiOC^tBu_2Ph$ with $TlPF_6$ forms the dimeric $Tl_2(OC^tBu_2Ph)_2$ complex, a rare example of a homoleptic thallium alkoxide complex demonstrating formally two-coordinate metal centers. Characterization of $Tl_2(OC^tBu_2Ph)_2$ by ^1H and ^{13}C NMR spectroscopy and X-ray crystallography reveals the presence of two isomers differing by the mutual conformation of the alkoxide ligands, and by the planarity of the central Tl-O-Tl-O plane. $Tl_2(OC^tBu_2Ph)_2$ serves as a convenient precursor to the formation of old and new $[M(OC^tBu_2Ph)_n]$ complexes (M = Cr, Fe, Cu, Zn), including a rare example of T-shaped $Zn(OC^tBu_2Ph)_2(THF)$ complex, which could not be previously synthesized using more conventional LiOR/HOR precursors. The reaction of $[Ru(cymene)Cl_2]_2$ with $Tl_2(OC^tBu_2Ph)_2$ results in the formation of a ruthenium(II) alkoxide complex. For ruthenium, the initial coordination of the alkoxide triggers C-H activation at the *ortho*-H of $[OC^tBu_2\mathit{Ph}]$ which results in its bidentate coordination. In addition to $Tl_2(OC^tBu_2Ph)_2$, related $Tl_2(OC^tBu_2(3,5\text{-}Me_2C_6H_3))_2$ was also synthesized, characterized, and shown to exhibit similar reactivity with iron and ruthenium precursors. Synthetic, structural, and spectroscopic characterizations are presented.

Introduction

Alkoxides are among the most ubiquitous ligands in coordination chemistry and homogeneous catalysis,[1-6] and therefore it is important to develop general, efficient, and reliable routes towards alkoxide-supported transition metal complexes. Two most common routes to the transition metal alkoxide complexes include salt metathesis between transition metal halide sources (MX_n) and alkali metal alkoxides (M'OR), or protonolysis of transition metal amide/alkyl precursors with more acidic alcohols.[7, 8] Both routes exhibit advantages and drawbacks. While the salt metathesis route employs commercially available transition metal halide precursors, it often yields mixed-metal "ate" complexes of $[MM'(OR)_nX]$ composition as a result of incomplete removal of M'X (M' = Li, Na, K).[1, 2, 9] In contrast, protonolysis route generally forms $M(OR)_n$ complexes cleanly. However, it requires the corresponding transition metal amide/alkyl precursors (often commercially unavailable). An alternative, less explored synthetic route to the metal-alkoxide complexes involves salt metathesis between thallium alkoxides TlOR and transition metal halides MX_n.[10, 11] As the reaction of TlOR with halide-containing complexes yields insoluble TlX salts, this route generally avoids formation of the mixed-metal species. This route also employs commercially available transition metal halide complexes; TlOR can be synthesized in one step using the combination of $TlPF_6$ (or other non-coordinating anion) with alkali metal alkoxides.

We have previously reported syntheses of mononuclear transition metal complexes supported by bulky alkoxide ligands OR (OR = $[OC^tBu_2Ph]$ and $[OC^tBu_2(3,5\text{-}Ph_2C_6H_3)]$), and their application in nitrene and carbene transfer reactions.[12] For M = Cr – Co, the reaction of MCl_2 with two equivalents of $LiOC^tBu_2Ph$ produced "seesaw clusters" of the $M_2Li_2Cl_2(OC^tBu_2Ph)_4$ form.[13] Subsequent treatment of these clusters with $TlPF_6$ yielded

$M(OC^tBu_2Ph)_2(THF)_2$ complexes for M = Mn, Fe, Co in moderate yields (overall yields between 30-40%).[14] For Cr, the second step of the procedure (treatment of $Cr_2Li_2Cl_2(OC^tBu_2Ph)_4$ with $TlPF_6$) failed to produce the desired chromium(II) bis(alkoxide) product. A different synthetic route, involving previously reported $Cr(N(SiMe_3)_2)_2(THF)_2$[15] (also synthesized from $CrCl_2$) was undertaken, and found to yield $Cr_2(OC^tBu_2Ph)_4$ dimer.[16] We hypothesized that the synthesis of $[M(OC^tBu_2Ph)_2]$ complexes can be improved by utilizing a single-step salt metathesis reaction of MCl_2 with $TlOC^tBu_2Ph$. Furthermore, our previous synthetic endeavors failed to produce $[Ni(OC^tBu_2Ph)_2]$ and $[Zn(OC^tBu_2Ph)_2]$ species, yielding unreactive $[M(OC^tBu_2Ph)_2(Cl)Li]$ complexes.[14, 17] It was hypothesized that the substitution of $LiOC^tBu_2Ph$ by $TlOC^tBu_2Ph$ would avoid the formation of stable heterobimetallic intermediates $[MM'(OC^tBu_2Ph)_nX]$ and would drive the reaction towards $[M(OC^tBu_2Ph)_2]$ species (and TlX). In this manuscript, we describe synthetic, spectroscopic and structural investigation of a new thallium complex with bulky alkoxide ligand $[OC^tBu_2Ph]$, which adopts a dimeric alkoxide-bridged structure $Tl_2(OC^tBu_2Ph)_2$. We also demonstrate that $Tl_2(OC^tBu_2Ph)_2$ can be used as a precursor in the synthesis of Cr, Fe, and Cu alkoxide complexes in one step, and leads to the previously inaccessible complexes with Zn and Ru.

Results and Discussion

Synthesis and characterization of $Tl_2(OC^tBu_2Ph)_2$

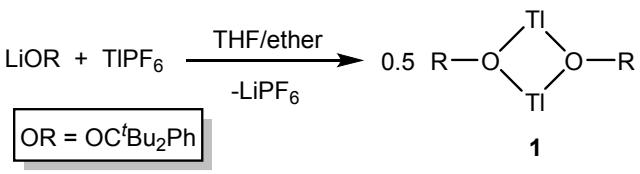

1

Scheme 1. Synthesis of $Tl_2(OC^tBu_2Ph)_2$ (**1**).

Mixing THF solutions of $TlPF_6$ and $LiOC^tBu_2Ph$[13] at room temperature produced silver-gray suspension that was stirred for 3 hours (Scheme 1). Subsequent solvent removal followed by recrystallization from hexane resulted in crystalline **1** in 56% yield (average of five experiments). **1** is stable in the solid state in the absence of light at -35 °C over at least one month. It slowly decomposes in solution as indicated by the formation of a silver precipitate. ^{1}H NMR spectrum of **1** (C_6D_6, room temperature) contained one dominant species (~90%) characterized by five broad aromatic and one aliphatic (^{t}Bu) signals, indicating a single type of [OC^tBu_2Ph] ligand with restricted phenyl rotation.[18] One of the aromatic signals overlapped with the solvent (benzene) peak, and was confirmed by homonuclear correlation spectroscopy (COSY). Close examination of ^{1}H NMR spectrum revealed the presence of additional, minor species (<10%) (^{t}Bu signal at 1.16 ppm, Figure S1 in ESI). Collecting ^{1}H NMR spectrum in toluene-d_8 demonstrated different (approximately 60:40) ratio between the two species, as indicated by two ^{t}Bu peaks at 1.23 and 1.16 ppm (Figure S3, ESI). A similar pattern was observed for the aromatic signals, most of which appear broad. Variable temperature (VT) NMR studies (toluene-d_8) demonstrated the presence of two isomers down to -40 °C (Figure 1); coalescence into single species was observed above room temperature. The isomers were assigned assuming that **1b** is a major isomer in both C_6D_6 and C_7D_8, and based on the fact that **1b** was isolated in a pure state and structurally characterized (see below).

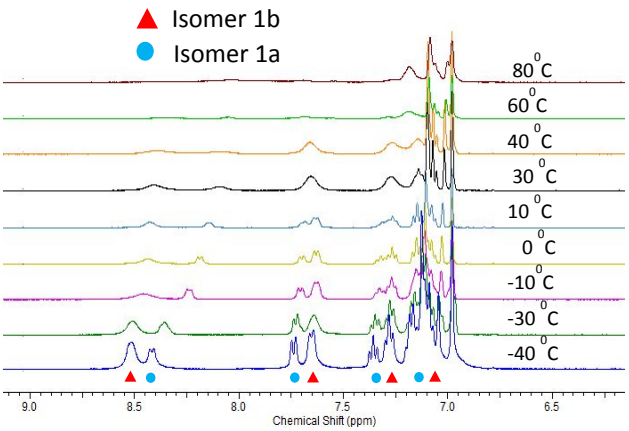

Figure 1. VT NMR (toluene-d_8, aromatic region) demonstrating the presence of two isomers of $Tl_2(OC^tBu_2Ph)_2$.

The X-ray crystallographic study rationalized spectroscopic observations revealing the presence of two structural isomers. The isomers were observed as two polymorphic structures (**1a** and **1b**) both adopting a dimeric $Tl_2(\mu\text{-}OC^tBu_2Ph)_2$ form (Figure 2). **1a** was obtained by recrystallization of $Tl_2(OC^tBu_2Ph)_2$ as prepared; crystals of **1b** were obtained in an attempt to make the $[Ni(OC^tBu_2Ph)_2]$ complex (see below). In both complexes, Tl(I) centers are formally two-coordinate. However, both complexes exhibit additional agostic interactions as indicated by the Tl···H-C distances in the range of 2.7 – 3.0 Å (see Figure S42 in ESI).[19] We note that formally two-coordinate dimeric homoleptic Tl alkoxides are exceedingly rare. Selected structures of homoleptic $[TlOR]_n$ complexes are given in Figure 3. For non-bulky alkoxides, TlOR usually adopt tetrameric cubane structures $[Tl(OR)]_4$ (in which Tl is three-coordinate),[20, 21] or lead to higher-nuclearity clusters $[Tl(OR)]_n$ (Tl featuring coordination number of 4 or higher).[22] Bulkier $[OC(CH_3)_3]$ and $[O(C(CF_3)_3)]$ ligands have been also shown to form tetrameric cubane structures $[Tl(OR)]_4$ featuring a three-coordinate Tl.[23, 24] In contrast, bulky 2,6-disubsituted aryloxides were shown to form dimeric formally two-coordinate $Tl_2(OAr)_2$

readily.[25-28] Less bulky aryloxides typically formed higher-nuclearity clusters or polymers,[29-32] except for the noteworthy example of electron-deficient aryloxides, such as in $Tl_2(O(p\text{-}C_6H_4F))_2$.[27]

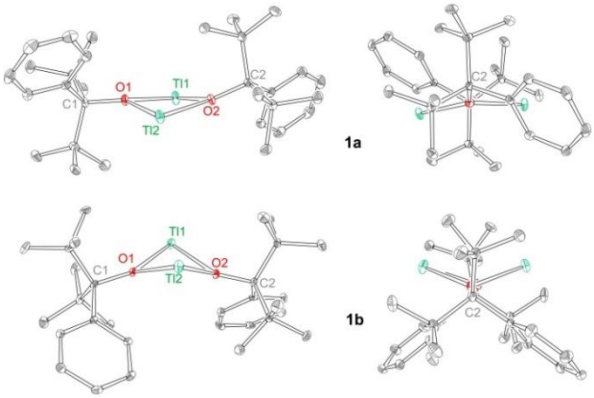

Figure 2. X-ray structures of two structural isomers of **1**, **1a** (top, side view and front view) and **1b** (bottom, side view and front view), 50% probability ellipsoids. H atoms are omitted for clarity. Selected bond distances (Å) for **1a**: Tl1-O1 2.389(2), Tl1-O2 2.402(2), Tl2-O2 2.396(2), Tl2-O1 2.399(2), Tl1--- Tl3.6647(4), O1---O2 3.045(2). Selected bond distances (Å) for **1b**: Tl1-O1 2.363(3), Tl1-O2 2.432(3), Tl2-O2 2.372(3), Tl2-O1 2.423(3), Tl1---Tl2 3.5646(3), O1---O2 2.922(3).

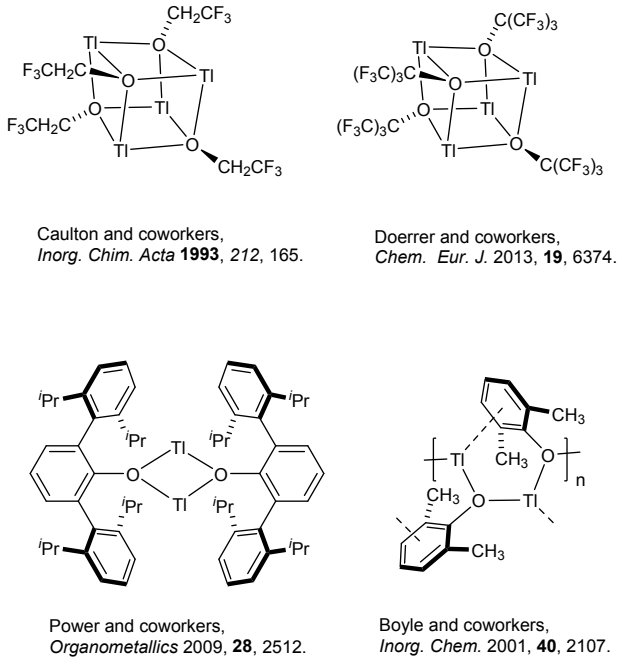

Figure 3. Selected examples of homoleptic TlOR/TlOAr structures.

While both **1a** and **1b** contain dimeric $Tl_2(\mu_2\text{-}OC^tBu_2Ph)_2$ structural units, there are notable differences between the structures. Most previously reported dimeric $Tl_2(OAr)_2$ structures exhibited planar, or nearly planar, Tl_2O_2 rings. Whereas **1a** displays only relatively small deviation from planarity (angle of 19° between Tl1-O1-Tl2 and Tl2-O2-Tl1 planes), the deviation from planarity in **1b** becomes more substantial (angle of 49° between Tl1-O1-Tl2 and Tl2-O2-Tl1 planes). What is the origin of the differences between torsion angles in **1a** and **1b**? Unlike aryloxides, which tend to have preferred conformation due to their planar nature, alkoxides (featuring three comparable substituents) are expected to be conformationally labile, especially when coordinated to a main-group element. Looking down the C1-C2 vector in **1a** reveals sterically favorable staggered conformation in **1a** (**Figure 2**, top right). In contrast, **1b** exhibits eclipsed conformation between the alkoxides substituents. Of the three substituents interacting between two different alkoxides (**Figure 2**, bottom right), two bottom substituents

exhibit less energetic anticlinal eclipsed relationship positioning ^{t}Bu on one half of **1b** in front of the phenyl on the other half. In contrast, two top ^{t}Bu are synperiplanar, which is the most sterically demanding interaction. To increase the distance between these two substituents, the angle between the Tl1-O1-Tl2 and Tl2-O2-Tl1 increases.

Alkoxide-transfer reactivity of $Tl_2(OC^tBu_2Ph)_2$

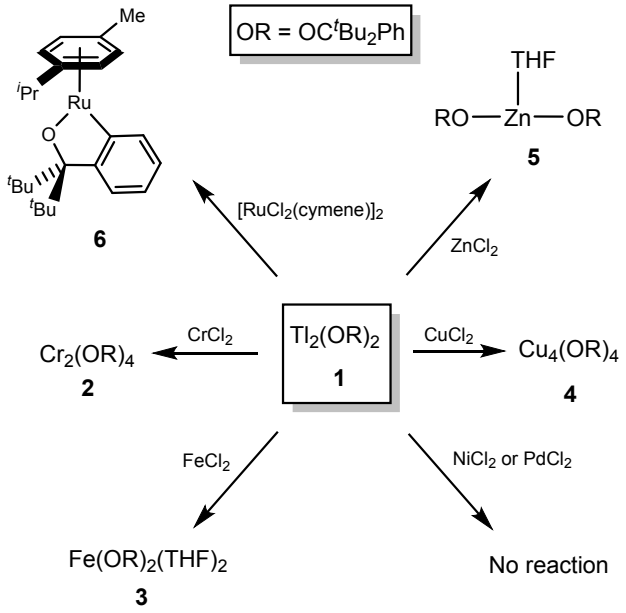

Scheme 2. Alkoxide-transfer reactions of $Tl_2(OC^tBu_2Ph)_2$ to obtain compounds **2**-**6**.

Following the synthesis and the characterization of $Tl_2(OC^tBu_2Ph)_2$, its potential as an alkoxide-transfer reagent with various transition metal chlorides was evaluated. Treatment of $CrCl_2$ and $FeCl_2$ with **1** produced previously reported complexes $Cr_2(OC^tBu_2Ph)_4$ (**2**, 64% yield)[16] and $Fe(OC^tBu_2Ph)_2(THF)_2$ (**3**, 51% yield).[33] Their compositions were confirmed by unit cell measurements and UV-vis spectra. The reaction of $CuCl_2$ with $Tl_2(OC^tBu_2Ph)_2$ produced the

Cu(I) product $Cu_4(OC^tBu_2Ph)_4$ (**4**, 39% yield), as previously observed for the reaction of $CuCl_2$ with $LiOC^tBu_2Ph$.[14]

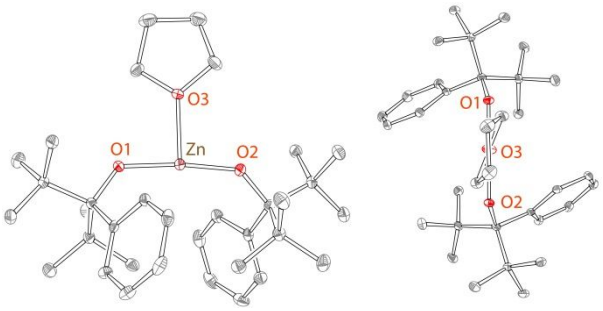

Figure 4. X-ray structure of **5**, 50% probability ellipsoids. H atoms are omitted for clarity. Selected bond distances (Å): Zn-O1 1.819(2), Zn-O2 1.825(2), Zn-O3 2.094(2). Selected bond angles (°): O1-Zn-O2 173.12(7), O1-Zn-O3 96.19(7), O2-Zn-O3 90.69(7).

We have also investigated the potential of $Tl_2(OC^tBu_2Ph)_2$ to form new bis(alkoxide) complexes, which could not be obtained previously via the $LiOC^tBu_2Ph/HOC^tBu_2Ph$ routes. Treatment of $NiCl_2$ with $Tl_2(OC^tBu_2Ph)_2$ resulted in the re-isolation of $Tl_2(OC^tBu_2Ph)_2$. These results are consistent with the previously observed lack of reactivity between $[Ni(OC^tBu_2Ph)(\mu\text{-}OC^tBu_2Ph)(\mu\text{-}Cl)Li(THF)_2]$ and $TlPF_6$.[14] Notably, a single isomer was observed in this case by ^1H NMR (Figure S17); crystal structure determination revealed the structure of **1b** (Figure 2). For Zn, we have previously reported that the reaction of $ZnEt_2$ with HOC^tBu_2Ph failed to produce the desired bis(alkoxide) complex, whereas treatment of $ZnCl_2$ with two equivalents of $LiOC^tBu_2Ph$ formed colorless $Zn(Cl)(\mu_2\text{-}OC^tBu_2Ph)_2Li(THF)$.[17] Treatment of $ZnCl_2$ with $Tl_2(OC^tBu_2Ph)_2$ yielded the new product **5**, which was obtained as colorless crystals from hexane (64% yield). The ^1H NMR characterization of **5** suggested formation of a zinc bis(alkoxide) tetrahydrofuran complex containing approximately a 2:1 ratio between $[OC^tBu_2Ph]$ and THF ligands.

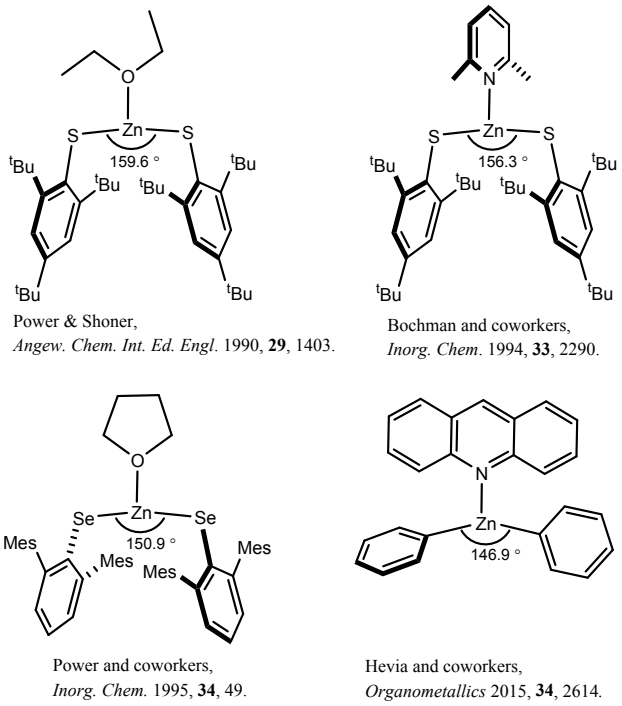

Power & Shoner, *Angew. Chem. Int. Ed. Engl*. 1990, **29**, 1403.

Bochman and coworkers, *Inorg. Chem*. 1994, **33**, 2290.

Power and coworkers, *Inorg. Chem.* 1995, **34**, 49.

Hevia and coworkers, *Organometallics* 2015, **34**, 2614.

Figure 5. Previously reported three-coordinate Zn complexes featuring geometry close to T-shape.

X-ray structure determination confirmed $Zn(OC^tBu_2Ph)_2(THF)$ composition for **5**. The structure (Figure 4) revealed T-shaped complex of approximate (non-crystallographic) C_2 symmetry. The alkoxide oxygens demonstrate nearly linear disposition (O1-Zn-O2 173.1(1)°), while the angles between alkoxides and the remaining THF ligands are close to 90° (see Figure 4 for structural details). Complex **5** is a rare example of a T-shaped Zn complex featuring alkoxide ligation. Cambridge Structural Database contains over 1000 examples of three-coordinate Zn complexes, of which only very few mononuclear examples demonstrated nearly T-shaped geometry (interligand angle of ~ 160°).[34-36] Several additional three-coordinate zinc complexes exhibited distorted trigonal geometries approaching T-shaped (angles ~ 150° or slightly below).[37-40] In contrast, alkoxide- (or aryloxide) ligated three-coordinate zinc complexes generally feature trigonal planar geometry.[17, 41-45] To the best of our knowledge, complex **3**

exhibits the most linear interligand RO-Zn-OR angle for any T-shaped mononuclear Zn complex.

We have also explored the reactivity of $Tl_2(OC^tBu_2Ph)_2$ towards heavier (4d) middle/late metals in the alkoxide ligand environment. This work specifically focused on M(II) complexes (M = Ru, Pd); complexes of both metals with unsupported alkoxide ligands are relatively rare.[1, 46-50] Treatment of $[RuCl_2(cymene)]_2$ with $Tl_2(OC^tBu_2Ph)_2$ resulted in the formation of a magenta solution, from which dark-purple crystals were isolated. ^{1}H NMR characterization of the crystalline product **6** (76% yield) demonstrated the presence of only four aromatic alkoxide signals, instead of the expected five phenyl protons of $[Tl_2(OC^tBu_2Ph)_2]$. In addition, the NMR spectrum contained cymene aromatic protons as two doublets at 5.17 and 5.05 ppm, one ^{t}Bu resonance (18 protons overall) at 1.18 ppm, cymene ^{i}Pr resonances at 1.02 and 2.09 ppm, and the cymene Me peak at 1.57 ppm. X-ray diffraction study disclosed the structure of C-H activated product **6** (Figure 6, left). **6** features bidentate coordination of the alkoxide through oxygen and the *ortho*-carbon to Ru(II) center, in addition to the η^6-bound cymene ligand. No reaction was observed between $PdCl_2$ and $Tl_2(OC^tBu_2Ph)_2$.

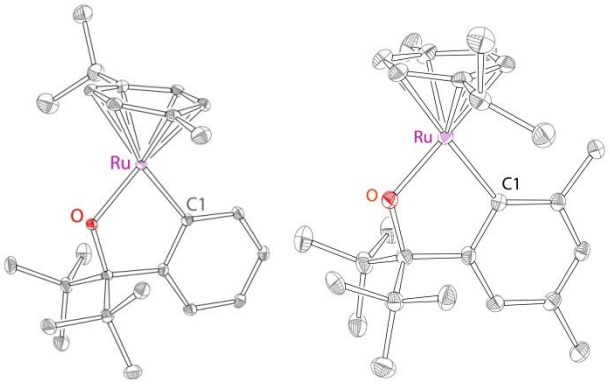

Figure 6. X-ray structures of **6** (left) and **10** (right), 50% probability ellipsoids. H atoms are omitted for clarity. Selected bond distances (Å) and angles (°) for **6**: Ru-O 1.933(2), Ru-C1

2.027(2), O-Ru-C1 80.94(7). Selected bond distances (Å) and angles (°) for **10**: Ru-O 1.910(1), Ru-C1 2.068(2), O-Ru-C1 81.32(5).

Synthesis and Reactions of $Tl_2(OC^tBu_2(3,5\text{-}Me_2C_6H_3))_2$

Thallium-mediated alkoxide-transfer protocol was explored with one additional bulky alkoxide ligand, [$OC^tBu_2(3,5\text{-}Me_2C_6H_3$]. $Tl_2(OC^tBu_2(3,5\text{-}Me_2C_6H_3))_2$ (**8**) was prepared by the reaction between $Li_2(OC^tBu_2(3,5\text{-}Me_2C_6H_3))_2(THF)_2$ (**7**, Figure S43) and $TlPF_6$ (Scheme 3) and obtained in 69% yield as colorless crystals. Similarly to $Tl_2(OC^tBu_2Ph)_2$, characterization of freshly crystallized $Tl_2(OC^tBu_2(3,5\text{-}Me_2C_6H_3))_2$ by ^1H NMR spectroscopy revealed the presence of two isomers (Figure S27). Notably, prolonged storage (4 weeks) of **8** in solution at -35 °C led to the formation of a single isomer (Figure S24), whose structure is shown in **Figure 7**. The structure of **8** is similar to **1b**, featuring non-planar Tl_2O_2 ring and (nearly) eclipsed conformation between the alkoxides. Similarly to **1**, **8** serves as a convenient precursor for the synthesis of transition metal alkoxide complexes. We specifically pursued two different reaction outcomes enabled by **1**, namely the formation of an iron bis(alkoxide) complex, and bidentate alkoxoaryl ruthenium complex. Treatment of **8** with $FeCl_2$ produced $Fe(OC^tBu_2(3,5\text{-}Me_2C_6H_3))_2(THF)_2$ (**9**, 61%) and the reaction of **8** with $[RuCl_2(cymene)]_2$ produced complex **10** (81%). The structures of **9** and **10** (Figures 8 and 6) are closely related to the structures of **3** and **6**; selected structural parameters are given in Figures 8 and 9.

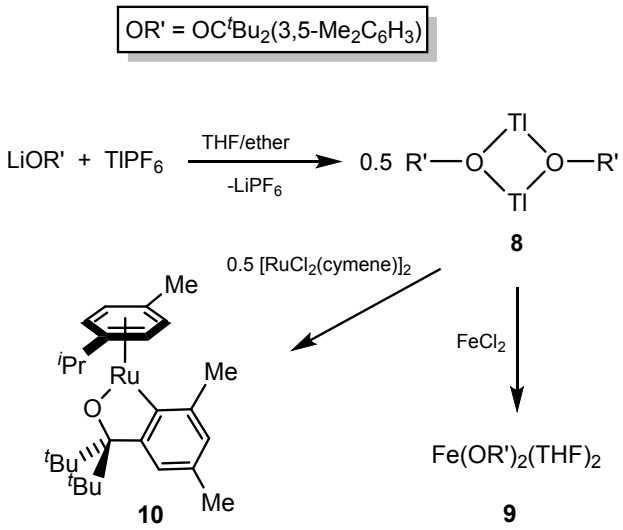

Scheme 3. Synthesis and reactivity of $Tl_2(OC^tBu_2(3,5\text{-}Me_2C_6H_3))_2$ (**8**)

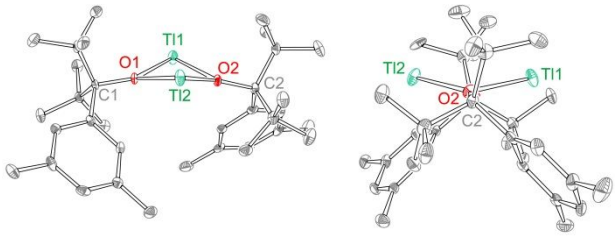

Figure 7. X-ray structures of **8** (side view and front view), 50% probability ellipsoids. H atoms are omitted for clarity. Selected bond distances (Å): Tl1-O1 2.361(4), Tl1-O2 2.394(4), Tl2-O2 2.366(4), Tl2-O1 2.406(4), Tl1--- Tl 3.6256(4), O1---O2 2.959(4).

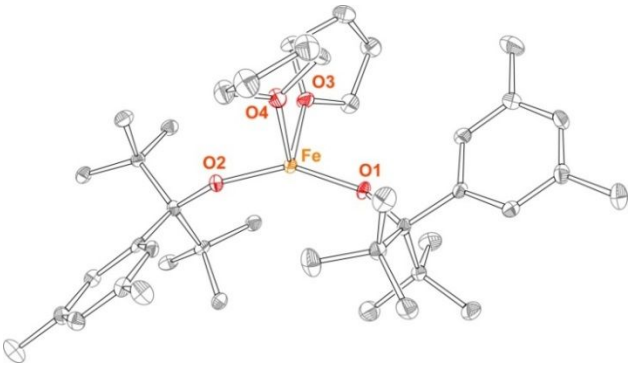

Figure 8. X-ray structure of **9**, 50% probability ellipsoids. H atoms are omitted for clarity. Selected bond distances (Å): Fe-O1 1.846(2), Fe-O2 1.851(2), Fe-O3 2.171(2), Fe-O4 2.232(2). Selected bond angles (°): O1-Fe-O2 148.1(1), O3-Fe-O4 88.8(1).

In summary, we have reported the synthesis of rare dimeric thallium-alkoxide complexes bearing bulky alkoxides [OC^{t}Bu$_2$Ph] and [OC^{t}Bu$_2$(3,5-Me$_2$C$_6$H$_3$)], Tl$_2$(OC^{t}Bu$_2$Ph)$_2$ and Tl$_2$(OC^{t}Bu$_2$(3,5-Me$_2$C$_6$H$_3$))$_2$. The complexes are observed as two different conformers; the distinct conformers are supported by VT ^{1}H NMR spectroscopy. Tl$_2$(OR)$_2$ precursors allow a one-step formation of transition metal complexes with bulky alkoxide ligands, [OC^{t}Bu$_2$Ph] and [OC^{t}Bu$_2$(3,5-Me$_2$C$_6$H$_3$)], which is generally more efficient and higher-yielding compared with the previously described two-step synthesis. Furthermore, the use of Tl$_2$(OC^{t}Bu$_2$Ph)$_2$ enabled preparation of the mononuclear T-shaped Zr(OC^{t}Bu$_2$Ph)$_2$(THF) species, as well as rare examples of the second-row complex (Ru) with both [OC^{t}Bu$_2$Ph] and [OC^{t}Bu$_2$(3,5-Me$_2$C$_6$H$_3$)]. In our future studies, we will continue exploring the reactivity of these and other Tl alkoxides (such as [OC^{t}Bu$_2$(3,5-Ph$_2$C$_6$H$_3$][51]) with the second- and third-row middle and late transition metals.

Experimental

General Methods and Procedures. All reactions involving air-sensitive materials were executed in a nitrogen-filled glovebox or by standard Schlenk line procedures. Nickel(II) chloride dimethoxyethane was purchased from Sigma-Aldrich. Thallium hexafluorophosphate and anhydrous chromium chloride were purchased from Strem. The synthesis of LiOC^{t}Bu$_2$Ph was reported previously.[13] All solvents were purchased from Fischer Scientific and were of

HPLC grade. The solvents were purified using an MBRAUN solvent purification system and stored over 3 Å molecular sieves. Deuterated benzene (C_6D_6) and toluene (C_7D_8) were purchased from Cambridge Laboratories, degassed under argon, and stored over 3 Å molecular sieves. NMR spectra were recorded at the Lumigen Instrument Center (Wayne State University). NMR was performed on Agilent 400 MHz or Agilent 600 MHz Spectrometers in C_6D_6 and C_7D_8 at room temperature unless otherwise noted. Chemical shifts and coupling constants (J) were reported in parts per million (δ) and hertz (Hz), respectively. IR spectra were recorded on Shimadzu IR-Affinityl FT-IR spectrometer as paratone oil mull suspensions. UV-Vis spectra were obtained using Shimadzu UV-1800 spectrometer.

Warning: Thallium hexafluorophosphate and other thallium salts are highly toxic, can be fatal if swallowed or inhaled and should be handled with utmost care! All reactions that involved thallium precursors or products were conducted in the glovebox. All thallium-contaminated waste (including glassware such as vials and pipets or kimwipes) was separated from the other glovebox waste and discarded separately labelled “thallium waste”.

X-ray Crystallographic Details. The structures of complexes **2**,[33] **3**,[16] and **4**[14] were reported previously. The structures of **1a**, **1b, 5-10** were determined by X-ray diffraction analysis. The crystals were mounted on a Bruker APEXII/Kappa goniometer platform diffractometer equipped with an APEX II detector. A graphic monochromator was employed for wavelength selection of the Mo Kα radiation (λ = 0.71073 Å). The data were processed and the structures were solved using the APEX 3 software supplied by Bruker AXS. The structures were refined with the program ShelXL using Olex2.[52, 53]. Hydrogen atoms were placed in calculated positions using a standard riding model and refined isotropically; all other atoms were refined anisotropically. The structure of **1b** exhibited high residual electron density in the vicinity of

heavy metal (Tl) centers, likely due to the imperfect absorption correction. The structure of **10** exhibited tert-butyl groups disorder which was successfully modeled by two alternating conformations. Selected crystal and structure refinement data is given in Table S1 (ESI).

Synthesis of $Tl_2(OC^tBu_2Ph)_2$ (1). A solution of $TlPF_6$ (100 mg, 0.287 mmol) in THF was added to a stirred clear ether solution of $LiOC^tBu_2Ph$ (63 mg, 0.276 mmol) at room temperature. The reaction turned silver-grey and was stirred at room temperature for three hours. The volatiles were removed *in vacuo*. The resulting solid was dissolved in hexane, filtered, and concentrated. Subsequent recrystallization at -35˚C yields X-ray quality crystals of **1** as two polymorphs **1a** and **1b** in 56% yield (average over five experiments, range between 49% and 62%). Scaled-up synthesis: A solution of $LiOC^tBu_2Ph$ (250 mg, 1.115 mmol) in ether was added to a stirred clear THF solution of $TlPF_6$ (400 mg, 1.152 mmol) at room temperature. The reaction turned silver-grey and was stirred at room temperature for three hours. The volatiles were removed in vacuo. The resulting solid was dissolved in hexane, filtered, and concentrated. Subsequent recrystallization at -35 ˚C yields X-ray quality crystals of **1** (218 mg, 46% yield). ^{1}H NMR (600 MHz, C_6D_6, room temperature) δ 8.52 (bs, 1H, Ph), 7.68 (bs, 1H, Ph), 7.29 (bs, 1H, Ph), 7.15 (bs, 1H, Ph), 7.10 (bs, 1H, Ph), 1.26 (s, 18H, Ph) ppm. ^{1}H NMR (400 MHz, C_7D_8, room temperature) δ 8.42 (bs, 1H, Ph), 8.10 (bs, 1H, Ph), 7.67 (bs, 2H, Ph), 7.27 (bs, 2H, Ph), 7.14 (t, $^3J_{HH}$ = 7 Hz, 2H, Ph), 7.09 (m, 2H, Ph), 1.23 (s, 18H), 1.16 (s, 10H) ppm. ^{1}H NMR (400 MHz, C_7D_8, -40 °C) δ 8.53 (bs, 1H, Ph), 8.44 (d, $^3J_{HH}$ = 6.7 Hz, 1H, Ph), 7.76 (d, $^3J_{HH}$ = 7.8 Hz, 1H, Ph), 7.68 (d, $^3J_{HH}$ = 7.4 Hz, 1H, Ph), 7.37 (t, $^3J_{HH}$ = 7.6 Hz, 1H, Ph), 7.30 (t, $^3J_{HH}$ = 7.2 Hz, 1H, Ph), 7.18 (m, 2H, Ph), 7.11 (m, 2H, Ph), 1.27 (s, 18H), 1.17 (s, 6H) ppm. ^{13}C NMR (C_6D_6, 150 MHz) δ 152.78, 130.59, 129.55, 126.53, 125.60, 125.36, 89.80, 43.62, 31.53 ppm. UV-vis: λ_{max}, nm (ε_M, L mol^{-1} cm^{-1}) 311 (3100), 294 (3300), 261 (sh, 6500).

Synthesis of $Cr_2(OC^tBu_2Ph)_4$ (2). A solution of $Tl_2(OC^tBu_2Ph)_2$ (70 mg, 0.083 mmol) in THF was added to a stirring THF solution of $CrCl_2$ (8 mg, 0.066 mmol) at room temperature. The reaction turned cloudy grey with a tinge of light green. The reaction was stirred at room temperature for 90 minutes. The volatiles were removed *in vacuo*. The resulting residue was dissolved in hexane, filtered, and concentrated. Subsequent recrystallization at -35˚C yields light green X-ray quality crystals of the previously characterized $Cr_2(OR)_4$[16] (21 mg, 64% yield).

Synthesis of $Fe(OC^tBu_2Ph)_2(THF)_2$ (3). A solution of $Tl_2(OC^tBu_2Ph)_2$ (190 mg, 0.222 mmol) in THF was added to a stirring THF solution of $FeCl_2$ (28 mg, 0.222 mmol) at room temperature. The solution color turned into brownish white. The reaction was stirred at room temperature for one hour. The volatiles were removed *in vacuo*. The resulting residue was dissolved in hexane, filtered, and concentrated. Recrystallization from hexane at -35˚C yielded white X-ray quality crystals of the previously synthesized $Fe(OC^tBu_2Ph)_2(THF)_2$[33] (72 mg, 51% yield). The nature of the product was confirmed by the unit cell measurements.

Synthesis of $Cu_4(OC^tBu_2Ph)_4$ (4). A solution of $Tl_2(OC^tBu_2Ph)_2$ (85 mg, 0.100 mmol) in THF was added to a stirring THF solution of $CuCl_2$ (13 mg, 0.10 mmol) at room temperature. The solution turned into deep red immediately and then into brown. The reaction was stirred at room temperature for one hour. The volatiles were removed *in vacuo*. The resulting residue was dissolved in hexane, filtered, and concentrated. Recrystallization from hexane at -35 ˚C yielded colorless crystals of the previously synthesized $Cu_4(OC^tBu_2Ph)_4$[14] (11 mg, 39% yield). The nature of the product was confirmed by ^1H NMR spectrum (see ESI).

Synthesis of $Zn(OC^tBu_2Ph)_2(THF)$ (5). A solution of $Tl_2(OC^tBu_2Ph)_2$ (170 mg, 0.200 mmol) in THF was added to a stirred THF solution of $ZnCl_2$ (27 mg, 0.200 mmol) at room temperature. The initially transparent solution turned into milky white suspension. The reaction

was stirred at room temperature for one hour. The volatiles were removed *in vacuo*. The residue was dissolved in hexane, filtered, and concentrated. Recrystallization from hexane at -35 ˚C yielded colorless crystals of **5** (74 mg, 64% yield). ^{1}H NMR (C_6D_6, 400 MHz) δ 7.92 (d, J_{HH} = 7.8 Hz, 2H, Ph), 7.65 (m, 2H, Ph), 7.18 (m, 2H, Ph), 7.09 (m, 4H, Ph), 3.73 (m, 4H, THF), 1.33 (m, 4H, THF), 1.23 (s, 36H) ppm. ^{13}C NMR (C_6D_6, 100 MHz) δ 151.25, 130.14, 127.89, 126.04, 125.94, 85.17, 69.66, 43.09, 31.58, 25.84 ppm. IR (cm^{-1}): 2970 (w), 2940 (w), 2878 (w), 2832 (w), 1489 (w), 1389 (w), 1366 (w), 1088 (w), 1057 (m), 988 (m), 748 (s), 710 (s).

Synthesis of Ru(cymene)(κ^2-OC^{t}Bu$_2$C$_6$H$_2$) (6). A solution of Tl_2(OC^{t}Bu$_2$Ph)$_2$ (85 mg, 0.100 mmol) in THF was added to a stirred THF solution of [Ru(*p*-cymene)Cl_2]$_2$ (31 mg, 0.050 mmol) at room temperature. Following the addition, the color of the solution turned magenta and precipitate formation was observed. The reaction was stirred at room temperature for one hour. The volatiles were removed *in vacuo*. The resulting residue was dissolved in hexane, filtered, and concentrated. Recrystallization from hexane at -35˚C yielded dark purple crystals of **6** (34 mg, 76% yield). ^{1}H NMR (C_6D_6, 600 MHz) δ 8.88 (d, J_{HH} = 7.6 Hz, 1H, Ph), 7.52 (d, J_{HH} = 7.9 Hz, 1H, Ph), 7.20 (t, J_{HH} = 7.2 Hz, 1H, Ph), 7.00 (m, 1H, Ph), 5.17 (d, J_{HH} = 5.6 Hz, 2H, cymene), 5.05 (d, J_{HH} = 5.6 Hz, 2H, cymene), 2.09 (m, 1H, cymene), 1.57 (s, 3H, cymene), 1.18 (s, 18H, ^{t}Bu), 1.02(d, J_{HH} = 5.9 Hz, 6H) ppm. ^{13}C NMR (C_6D_6, 150 MHz) δ 178.44, 168.41, 139.79, 124.45, 124.08, 122.31, 106.74, 96.84, 84.48, 81.77, 80.43, 39.33, 32.24, 31.03, 23.09, 19.99 ppm. UV-vis: λ_{max}, nm (ε_M, L mol^{-1} cm^{-1}): 539 (2800), 355 nm (8600), 296 nm (sh, 13400), 256 nm (28300). Anal. Calcd for C25H36ORu•0.5H2O: C, 64.90; H, 8.06. Found: C, 64.86; H, 7.77.

Synthesis of LiOC^{t}Bu$_2$(3,5-Me$_2$C$_6$H$_3$) (7). To a solution of 1-bromo-3,5-dimethylbenzene (0.430 g, 2.33 mmol) in 4 ml ether and 2 ml THF, a solution of t-BuLi in

pentane (2.7 ml, 1.7 M) was added dropwise at -35 °C. The solution changed color from colorless to yellow. The reaction was allowed to slowly warm to room temperature while stirred for one hour, after which it was cooled again to -35 °C and added to a cold solution of hexamethylacetone (0.4 mL, 2.31 mmol) in 2 ml of ether. The reaction was stirred for 24 hours, after which all solvents were removed under in vacuo to yield yellowish white residue. The residue was dissolved in hexanes and kept at -35 °C to get colorless crystals of **7** (428 mg, 81% yield). ^{1}H NMR (600 MHz, C_6D_6, room temperature) δ 7.67 (s, 1H, Ph), 7.43 (s, 1H, Ph), 6.75 (s, 1H, Ph), 2.30 (s, 3H, Me), 2.19 (s, 3H, Me), 1.19 (s, 18H, ^{t}Bu) ppm. ^{13}C NMR (C_6D_6, 150 MHz) δ 152.80, 137.63, 136.02, 125.46, 85.46, 43.04, 32.05, 22.42 ppm. IR (cm^{-1}): 2962 (m), 2870 (m), 2816 (w), 1604(w), 1481 (w), 1388 (w), 1365 (w), 1126 (w), 1080 (s), 1010 (m), 849 (s), 764 (s), 709 (s). The structure of **7** was also confirmed by the X-ray structure determination (see ESI).

Synthesis of $Tl_2(OCBu_2(3,5\text{-}Me_2C_6H_3))_2$ (8). A solution of $TlPF_6$ (89 mg, 0.255 mmol) in THF was added to a stirred clear THF solution of $LiOC^{t}Bu_2(3,5\text{-}Me_2Ph)$ (65 mg, 0.256 mmol) at room temperature. The reaction turned silver-grey and was stirred at room temperature for two hours. The volatiles were removed *in vacuo*. The resulting solid was dissolved in hexane, filtered, and concentrated. Subsequent recrystallization at -35 °C yields colorless crystals of **8** (79 mg, 69% yield). ^{1}H NMR (600 MHz, C_6D_6, room temperature) δ 8.14 (bs, 1H, Ph), δ 7.42 (bs, 1H, Ph), δ 6.74 (bs, 1H, Ph), δ 2.25 (s, 6H, Me) δ 1.26 (s, 18H, ^{t}Bu) ppm. ^{13}C NMR (C_6D_6, 150 MHz) δ 153.35, 136.17, 135.52, 129.69, 128.84, 127.89, 90.42, 44.65, 32.65, 22.66 ppm. UV-vis: λ_{max}, nm (ε_M, L mol^{-1} cm^{-1}) 316 (900), 297 (1200). The structure of **8** was also confirmed by the X-ray structure determination.

Synthesis of Fe(OC^{t}Bu$_2$(3,5-Me$_2$C$_6$H$_3$))$_2$(THF)$_2$ (9). A solution of Tl$_2$(OC^{t}Bu$_2$(3,5-Me$_2$C$_6$H$_3$))$_2$ (190 mg, 0.210 mmol) in THF was added to a stirred THF solution of FeCl$_2$ (27 mg, 0.210 mmol) at room temperature. The solution color turned into light brown, and white precipitate formation was observed. The reaction was stirred at room temperature for one hour. The volatiles were removed *in vacuo*. The resulting residue was dissolved in hexane, filtered, and concentrated. Recrystallization from hexane at -35 °C yielded light yellow X-ray quality crystals of **9** (82 mg, 61% yield). UV-vis: λ_{max}, nm (ε_M, L mol^{-1} cm^{-1}) 407 (sh, 250). IR (cm^{-1}): 2970 (w), 2978 (m), 2885 (m), 2831 (w), 1597 (w), 1481 (w), 1388 (w), 1350 (w), 1134 (m), 1087 (s), 1033 (s), 894 (m), 848 (s), 763 (m), 702 (s). The structure of **9** was also confirmed by the X-ray structure determination. Anal. Calcd for C42H70FeO4•H2O: C, 70.76; H, 10.18. Found: C, 69.92; H, 9.78.

Synthesis of Ru(cymene)[(κ^2-OC^{t}Bu$_2$Me$_2$C$_6$H$_2$)] (10). A solution of Tl$_2$(OC^{t}Bu$_2$(3,5-Me$_2$C$_6$H$_3$))$_2$ (133 mg, 0.147 mmol) in THF was added to a stirred THF solution of [Ru(*p*-cymene)Cl$_2$]$_2$ (45 mg, 0.074 mmol) at room temperature. Following the addition, the solution turned magenta and precipitate formation was observed. The reaction was stirred at room temperature for one hour. The volatiles were removed in vacuo. The resulting residue was dissolved in hexane, filtered, and concentrated. Recrystallization from hexane at -35˚C yielded dark purple X-ray quality crystals of **10** (59 mg, 81% yield).^{1}H NMR (C$_6$D$_6$, 600 MHz) δ 7.27 (s, 1H, Ph), 7.01 (s, 1H, Ph), 5.55 (d, J_{HH} = 6.2 Hz, 2H, cymene), 5.42 (d, J_{HH} = 6.2 Hz, 2H, cymene), 3.09 (s, 3H, Me), 2.21 (s, 3H, Me), 1.57 (s, 3H, Me), 1.95 (sept, J_{HH} = 6.7 Hz, 1H, ^{i}Pr), 1.43 (s, 3H, Me) 1.20 (s, 18H, ^{t}Bu), 0.97 (d, J_{HH} = 6.7 Hz, 6H, ^{i}Pr) ppm. ^{13}C NMR (C$_6$D$_6$, 150 MHz) δ 176.88, 171.10, 149.55, 131.34, 127.73, 123.06, 106.48, 90.20, 84.55, 82.99, 78.88, 39.96, 32.54, 31.45, 30.56, 23.37, 22.35, 20.44 ppm. UV-vis: λ_{max}, nm (ε_M, L mol^{-1} cm^{-1}): 545

(5200), 361 (15400), 263 (30000). The structure of **10** was also confirmed by the X-ray structure determination.

Electronic supplementary information (ESI) available: NMR, IR and UV-vis spectra. CCDC 2044386-2044389 and 2053857-2053860.

Conflicts of interest

There are conflicts of interest to declare.

Acknowledgements

S. G. is grateful to the National Science Foundation (NSF) for current support under grant number CHE-1855681. Experimental characterization was carried out at Lumigen Instrument Center of Wayne State University. We thank Ms. Hashini N. Munasinghe for the experimental assistance. Duleeka Wannipurage is a Rumble Fellow.

References

1. D. C. Bradley, R. C. Mehrotra, I. Rothwell, A. Singh, Alkoxo and Aryloxo Derivatives of Metals; Academic Press: London, UK, 2001

2. N. Y. Turova, E. P. Turevskaya, V. G. Kessler, M. I. Yanovskaya, The Chemistry of Metal Alkoxides; Springer: New York, NY, 2002.

3. R. C. Mehrotra, A. Singh and S. Sogani, *Chem. Soc. Rev*., 1994, **23**, 215-225.

4. R. R. Schrock and C. Copéret *Organometallics*, 2017, **36**, 1884-1892.

5. R. R. Schrock, "High Oxidation State Molybdenum and Tungsten Complexes Relevant to Olefin Metathesis" In Handbook of Metathesis, Vol 1, 2nd Ed., Wiley-VCH, Weinheim, R. H. Grubbs and A. G. Wenzel, Ed., 2015, pp. 1-32.

6. S. E. N. Brazeau and L. H. Doerrer, *Dalton Trans.,* 2019, **48**, 4759-4768.

7. P. T. Wolczanski, *Polyhedron*, **1995**, *14*, 3335–3362.

8. J. A. Bellow, M. Yousif, S. Groysman, *Comments Inorg. Chem*., **2015**, *36*, 92-122.

9. K. G. Caulton and L. G. Hubert-Pfalzgraf, *Chem. Rev*. 1990, **90**, 969–995.

10. M. V. Petersen, A. H. Iqbal, L. N. Zakharov, A. L. Rheingold and L. H. Doerrer, *Polyhedron*, 2013, **52**, 276-283.

11. J. S. Lum, P. E. Chen, A. L. Rheingold and L. H. Doerrer, *Polyhedron*, 2013, **58**, 218-228.

12**.** A. Grass, D. Wannipurage, R. L. Lord and S. Groysman, *Coord. Chem. Rev.*, 2019, **400**, 1-16.

13. J. A. Bellow, D. Fang, N. Kovacevic, P. D. Martin, J. Shearer, G. A. Cisneros and S. Groysman, *Chem. Eur. J*., 2013, **19**, 12225-12228.

14. J. A. Bellow, M. Yousif, D. Fang, E. G. Kratz, G. A. Cisneros and S. Groysman, *Inorg. Chem*., 2015, **54**, 5624-5633.

15. D. C. Bradley, M. B. Hursthouse, C. W. Newing and A. J. Welch, *J. Chem. Soc., Chem. Commun*., 1972, 567−568.

16. M. Yousif, D. J. Tjapkes, R. L. Lord and S. Groysman, *Organometallics*, 2015, **34**, 5119-5128.

17**.** T. S. Hollingsworth, R. L. Hollingsworth, T. Rosen and S. Groysman, *RSC Adv*., 2017, **7**, 41819-41829.

18. D. Wannipurage, T. S. Hollingsworth, F. Santulli, M. Cozzolino, M. Lamberti, S. Groysman and M. Mazzeo, *Dalton Trans.*, 2020, **49**, 2715-2723.

19. V. Kumar, V. Singh, A. N. Gupta, M. G. B. Drew and N. Singh, *Dalton Trans*., 2015, **44**, 1716-1723.

20. H. Rothfuss, K. Folting and K. G. Caulton, *Inorg. Chim. Acta*, 1993, **212**, 165-173.

21. C. A. Zechmann, T. J. Boyle, D. M. Pedrotty, T. M. Alam, D. P. Lang, B. L. Scott, *Inorg. Chem*., 2001, **40**, 2177-2184.

22. T. J. Boyle, C. A. Zechmann, T. M. Alam, M. A. Rodriguez, C. A. Hijar and B. L. Scott *Inorg. Chem*., 2002, **41**, 946-957.

23. F. Blasberg, H.-W. Lerner and M. Bolte, *Acta Crystallogr. Sect. E: Struct. Rep. Online*, **2010**, 66, m1621, DOI: 10.1107/S1600536810047550.

24. J. S. Lum, L. Tahsini, J. A. Golen, C. Moore, A. L. Rheingold and L. H. Doerrer, *Chem. Eur. J*., 2013, **19**, 6374-6384.

25. H. W. Roesky, M. Scholz, M. Noltemeyer and F. T. Edelmann, *Inorg. Chem*., 1989, **28**, 3829-3830.

26. Z. Zhu, R. J. Wright, Z. D. Brown, A. R. Fox, A. D. Phillips, A. F. Richards, M. M. Olmstead and P. P. Power, *Organometallics*, 2009, **28**, 2512-2519.

27. K. Akhbari and A. Morsali, *CrystEngComm*, 2012, **14**, 1618-1628.

28. A. A. El-Hadad, J. E. Kickham, S. J. Loeb, L. Taricani and D. G. Tuck, *Inorg. Chem*., 1995, **34**, 120-123.

29. K. Akhbari and A. Morsali, *Polyhedron*, 2011, **30**, 2459-2465.

30. M. V. Childress, D. Millar, T. M. Alam, K. A. Kreisel, G. P. A. Yap, L. N. Zakharov, J. A. Golen and A. L. Rheingold, L. H. Doerrer, *Inorg. Chem*., 2006, **45**, 3864-3872.

31. J. M. Harrowfield, R. P. Sharma, B. W. Skelton and A. H. White, *Aust. J. Chem*., 1998, **51**, 735-746.

32. A. Askarinejad and A. Morsali, *Inorg. Chem. Commun*., 2006, **9**, 143-146.

33. J. A. Bellow, P. D. Martin, R. L. Lord, S. Groysman, *Inorg. Chem.*, 2013, **52**, 12335 -12337.

34. P. P. Power and S. C. Shoner, *Angew. Chem. Int Ed. Engl*., 1990, **29**, 1403-1404.

35. M. Bochmann, G. C. Bwembya, R. Grinter, A. K. Powell, K. J. Webb, M B. Hursthouse, K. M. Abdul Malik and M. A. Mazid. *Inorg. Chem*., **1994**, *33*, 2290-2296.

36. M. Westerhausen, B. Rademache and W. Schwarz, *Z. Anorg. Allg. Chem*., 1993, **619**, 675-689.

37. E. Martin, D. L. Hughes and S. J. Lancaster, *Eur. J. Inorg. Chem.*, 2006, 4037–4041.

38. J. J. Ellison, K. Ruhlandt-Senge, H. H. Hope and P. P. Power, *Inorg. Chem*., 1995, **34**, 49-54.

39. G. Zhu, J. M. Tanski and G. Parkin *J. Chem. Crystallogr.*, 2002, **32**, 469-475.

40. A. Hernán-Gómez, E. Herd, M. Uzelac, T. Cadenbach, A. R. Kennedy, I. Borilovic, G. Aromı́, and E. Hevia *Organometallics*, 2015, **34**, 2614−2623.

41. G. Anantharaman and K. Elango, *Organometallics*, 2007, **26**, 1089-1092.

42. D. J. Darensbourg, S. A. Niezgoda, J. D. Draper and J. H. Reibenspies, *Inorg. Chem.*, 1999, **38**, 1356-1359.

43. D. J. Darensbourg, M. S. Zimmer, P. Rainey and D. L. Larkins, *Inorg. Chem*., **1998**, *37*, 2852-2853.

44. P. Jochmann and D. W. Stephan, *Chem. Eur. J*., 2014, **20**, 8370–8378.

45. S. A. Cantalupo, J. S. Lum, M. C. Buzzeo, C. Moore, A. G. Di Pasquale, A. L. Rheingold, L. H. Doerrer, *Dalton Trans*., 2010, **39**, 374-383.

46. J. R. Fulton, A. W. Holland, D. J. Fox and R. G. Bergman, *Acc. Chem. Res*., 2002, **35**, 44–56.

47. M. S. Sanford, L. M. Henling, M. W. Day and R. H. Grubbs, *Angew. Chem. Int. Ed*., 2000, **39**, 3451-3453.

48. C. Melero, L. M. Martınez-Prieto, P. Palma, D. del Rio, E. A. lvareza and J. Campora, *Chem. Commun.*, 2010, **46**, 8851–8853.

49. C. C. Comanescu and V. M. Iluc, *Organometallics*, 2014, **33**, 6059-6064.

50. I. Matas, J. Cámpora, P. Palma and E. Álvarez, *Organometallics*, 2009, **28**, 6515−6523.

51. M. Yousif, D. Wannipurage, C. D. Huizenga, E. Washnock-Schmid, N. J. Peraino, A. Ozarowski, S. A. Stoian, R. L. Lord and S. Groysman, *Inorg. Chem*., 2018, **57**, 9425-9438.

52. G. M. Sheldrick, *Acta Cryst*., 2015, *C71*, 3-8.

53. O. V. Dolomanov, L. J. Bourhis, R. J. Gildea, J. A. K. Howard and H. Puschmann, *J. Appl. Cryst*. 2009, **42**, 339-341.